Published OnlineFirst March 10, 2009; DOI: 10.1158/1541-7786.MCR-08-0409

Comparative Analysis of DNA Repair in Stem and Nonstem Glioma Cell Cultures

Monica Ropolo,[1] Antonio Daga,[2] Fabrizio Griffero,[2] Mara Foresta,[1] Gianluigi Casartelli,[1] Annalisa Zunino,[3] Alessandro Poggi,[4] Enrico Cappelli,[5] Gianluigi Zona,[6] Renato Spaziante,[6] Giorgio Corte,[2,7] and Guido Frosina[1]

[1]Molecular Mutagenesis and DNA Repair, [2]Gene Transfer, [3]Cytogenetics, and [4]Immunology Laboratories, Istituto Nazionale Ricerca Cancro; [5]Department of Pediatric Hemato-Oncology, Istituto Giannina Gaslini; [6]Section of Neurosurgery, Department of Neuroscience, Ophthalmology and Genetics, and [7]Department of Oncology Biology and Genetics, University of Genova, Genova, Italy

Abstract

It has been reported that cancer stem cells may contribute to glioma radioresistance through preferential activation of the DNA damage checkpoint response and an increase in DNA repair capacity. We have examined DNA repair in five stem and nonstem glioma cell lines. The population doubling time was significantly increased in stem compared with nonstem cells, and enhanced activation of Chk1 and Chk2 kinases was observed in untreated CD133$^+$ compared with CD133$^-$ cells. Neither DNA base excision or single-strand break repair nor resolution of pH2AX nuclear foci were increased in CD133$^+$ compared with CD133$^-$ cells. We conclude that glioma stem cells display elongated cell cycle and enhanced basal activation of checkpoint proteins that might contribute to their radioresistance, whereas enhanced DNA repair is not a common feature of these cells.
(Mol Cancer Res 2009;7(3):383–92)

Introduction

Appreciating the biological distinctness of glioma stem cells is crucial for the development of specific therapies that effectively target these cells in patients and improve treatment outcome (1). Resistance of glioma stem cells to chemotherapeutic drugs has been reported (2) and an expression signature dominated by HOX genes, which comprises the CD133 stem cell antigen, emerged as a predictor for poor survival in glioma patients treated with concomitant chemoradiotherapy (3). Expression of antiapoptotic and multidrug resistance-associated protein genes has been found elevated in cancer stem-like cells isolated from glioblastoma and astrocytoma and may represent important mechanisms of resistance to chemotherapy and radiotherapy in these cells (4). Overexpression of multiple ion channel genes (e.g., chloride intracellular channel 1) may also contribute to resistance of glioma stem cells to alkylating agents (5). Hence, different mechanisms may underlie resistance of glioma stem cells to radiotherapeutic and chemotherapeutic agents. The contribution of DNA repair to this clinically decisive phenomenon is poorly defined. Bao et al. (6) have proposed that glioma stem cells may resist radiation through preferential activation of the DNA damage checkpoint response and an increase in DNA repair capacity. In this study, the fraction of tumor cells expressing CD133 was enriched after radiation in gliomas. In both cell culture and brains of immunocompromised mice, CD133$^+$ glioma cells survived ionizing radiation (IR) in increased proportions relative to most tumor cells, which lack CD133. CD133$^+$ tumor cells isolated from both human glioma xenografts and primary patient glioblastoma specimens preferentially activated the DNA damage checkpoint in response to radiation and repaired IR-induced DNA damage more effectively than CD133$^-$ tumor cells (6). In addition, the radioresistance of CD133$^+$ glioma stem cells could be reversed with a specific inhibitor of the Chk1 and Chk2 checkpoint kinases. To improve our knowledge on the role of DNA repair in resistance of glioma stem cells, we have examined the DNA repair capacity of five stem cell lines, as defined by Vescovi et al. (7), in comparison with five established nonstem glioma cell lines. The population doubling time (PDT) was significantly increased in the stem lines and activation of the checkpoint kinases Chk1 and Chk2 was more pronounced in untreated CD133$^+$ compared with CD133$^-$ cells. We could not find any significant increase of DNA base excision repair (BER), single-strand break (SSB) repair, and resolution of pH2AX foci, an indicator of double-strand break (DSB) repair.

Results

Characterization of Glioma Stem Cells

It was pursued following criteria proposed by Vescovi et al. (7).

Extensive Self-Renewal Ability. We analyzed stem and nonstem cell lines for expression of stem markers CD133 and

Received 8/29/08; revised 11/14/08; accepted 12/2/08; published OnlineFirst 3/10/09.
Grant support: Compagnia di S. Paolo, Programma "Oncologia," Italian Ministry of University and Research, "Fondo Investimenti Ricerca Base Internazionalizzazione," and Istituto Superiore Sanità, Programma Italia-USA "Malattie Rare" (G. Frosina) and Fondazione Carige and Italian Ministry of Health (G. Corte).
The costs of publication of this article were defrayed in part by the payment of page charges. This article must therefore be hereby marked *advertisement* in accordance with 18 U.S.C. Section 1734 solely to indicate this fact.
Note: M. Ropolo, A. Daga, G. Corte and G. Frosina contributed equally to this work.
Requests for reprints: Guido Frosina, Molecular Mutagenesis and DNA Repair Laboratory, Istituto Nazionale Ricerca Cancro, Largo Rosanna Benzi n. 10, 16132 Genova, Italy. Phone: 39-105737543; Fax: 39-105737237. E-mail: guido.frosina@istge.it

doi:10.1158/1541-7786.MCR-08-0409

Published OnlineFirst March 10, 2009; DOI: 10.1158/1541-7786.MCR-08-0409

nestin as well as their population kinetics and cell cycle distribution *ex vivo* (7). Glioma subpopulations expressing CD133 are enriched for cancer stem cells and show elevated tumorigenic potential (8-10), although it is still unclear which subset of the $CD133^+$ precursor pool can initiate tumor formation *in vivo* and the existence of $CD133^-$ cancer stem cells has been shown as well (7-10). The five stem cultures investigated in this study (Fig. 1A, *solid columns*, and C) expressed CD133 at variable extent ranging from 1% (2/11) to 85% (BORRU) of cells (average ± SE, 26 ± 16%). All stem cell cultures further expressed the stem marker nestin (Fig. 1B and D) at relatively high levels, ranging from 40% (BORRU) to 100% (PERU and 2/11) of cells (average ± SE, 85 ± 11%). The population kinetics of stem cells was analyzed by determining their PDT and cell cycle distribution. The PDT of stem glioma cells are shown in Fig. 1E. Stem cells (Fig. 1E, *left, solid columns*) displayed an average 58 ± 2 h PDT and maintained extensive cell renewal ability with unchanged proliferation parameters over a period of at least 3 months of continuing culture (data not shown). Analysis of cell cycle distribution (Fig. 1F, *left*) showed 54% of cells in G_0-G_1 and 28% in apoptosis.

No nonstem cell line expressed CD133 (Fig. 1A and C). Remarkably, the A172 and U373 cell lines that maintain proliferative capacity under stem culture conditions [presence of epidermal growth factor (EGF)-fibroblast growth factor (FGF) and absence of FCS] expressed elevated levels of nestin (90% of positive cells; Fig. 1B and D; average ± SE for nonstem cells, 37 ± 21%). Thus, expression of nestin correlates with the ability to proliferate under stem culture conditions but not with cancer-initiating ability (see below; Table 1). Nonstem cell lines (Fig. 1E, *open columns*) displayed a significant 1.9-fold lower PDT (average ± SE, 31 ± 5 h) compared with stem cells. No significant difference in cell cycle distribution or apoptosis was observed between stem and nonstem cell lines (Fig. 1F). The cell renewal ability of immortalized, established nonstem cell lines is by definition unlimited.

Cancer-Initiating Ability on Orthotopic Implantation. When 10^5 cells are injected orthotopically in immunodeficient mice, all stem cell lines produce a tumor histologically very similar (phenocopy) to the original tumor (Table 1; Fig. 1G). Nonstem established cell lines are also capable to cause tumor development when implanted orthotopically, although the number of cells to be injected in athymic mice may vary widely (11-15). The A172 cell line is nontumorigenic (11-14). Hence, cancer-initiating ability on orthotopic implantation is not a hallmark of brain cancer stem cells only.

Karyotypic Alterations. The karyotypes of stem cell lines showed chromosomal alterations (Table 2). Structural aberrations were lower in stem cell lines (total, 18) than in nonstem cell lines (total, 44), whereas numerical aberrations were similar in stem and nonstem cells (49 and 52, respectively; Table 2). The average numbers of spontaneous (Fig. 2A) or temozolomide- and IR-induced (Fig. 2B and C) micronuclei did not differ significantly in stem and nonstem cells.

Capacity to Generate Nontumorigenic End Cells. We sorted $CD133^+$ cells in stem lines and confirmed that they have greater tumorigenic capacity than $CD133^-$ cells (Table 3). 10^4 $CD133^+$ cells (10^3 in the case of COMI) were sufficient to drive tumor growth in immunodeficient mice, whereas 10^5 $CD133^-$ cells of any cell line failed. All five stem populations thus included $CD133^-$ cells with low/null tumorigenic potential. No suitable marker for separation of tumorigenic and nontumorigenic cells was available in nonstem cell lines. Although with different potential, four of five of them are capable to sustain tumor growth when implanted orthotopically (Table 1). Nevertheless, all of them are negative for CD133 as determined with our FACSCalibur system (Fig. 1A and C). This indicates that CD133 may not be a suitable marker of tumorigenicity in nonstem cell lines. To our knowledge, no marker is currently available to sort tumorigenic from nontumorigenic cells in established nonstem glioma cell lines.

Differentiation Capacity. This was the only parameter that unequivocally permitted, in our hands, to distinguish stem from nonstem glioma cells. Stem cells were cultured in this study as adherent monolayers, allowing convenient morphologic analysis of differentiation under the inverted light microscope (Fig. 3). Removal of growth factors and addition of FCS (differentiating conditions) resulted after 3 weeks in acquisition of a typical astroglial morphology by the five stem cell lines (Fig. 3A, *STEM-FCS*). Analysis of marker expression confirmed the morphologic analysis (Fig. 3B). Glial fibrillary acidic protein (GFAP) is an intermediate filament protein that is highly specific for cells of astroglial lineage. The percentage of $GFAP^+$ cells (Fig. 3B; average, 29 ± 14%) significantly increased under differentiating conditions (Fig. 3B; average, 81 ± 7%), indicating that differentiation of stem cultures was mostly oriented to astroglial commitment.

In adult tissues, the distribution of β-tubulin III is almost exclusively neuron specific, making this protein a useful marker of neural differentiation. The percentage of stem cells expressing β-tubulin III (Fig. 3C; average, 70 ± 11%) was unchanged under differentiating conditions (Fig. 3C; average, 70 ± 9%), indicating that stem cultures used in this study do not commit to neuronal differentiation on removal of growth factors.

On differentiation (Fig. 3D), the average PDT significantly increased from 58 ± 2 to 83 ± 8 h, indicating that differentiation involves a decreased rate of proliferation. Analysis of cell cycle distribution and apoptosis by fluorescence-activated cell sorting (Fig. 3E) showed no accumulation of differentiating cells in any particular phase of the cell cycle nor increased apoptosis. Hence, differentiation does not imply a cell cycle block at a specific point or increased programmed cell death but rather an elongation of all phases of the cell cycle.

The morphology of nonstem glioma cell lines is shown in Fig. 3A (*Non-STEM*). Normally, these cells are cultured in the presence of FCS and Matrigel coating of flasks is dispensable for their proliferation. Under stem cell culture conditions (*EGF-FGF*), proliferation of some cell lines (D54, U87, and U251) was suppressed, whereas the proliferation rate of A172 and U373 was essentially unchanged. Matrigel coating of flasks was indispensable for proliferation of A172 and U373 in EGF-FGF. Nonstem cell lines could never acquire an astroglial-like morphology (Fig. 3A, *Non-STEM-FCS*) and no GFAP expression was observed in them with the exception of the U373 cell line where a limited number of $GFAP^+$ cells was counted (data not shown).

Published OnlineFirst March 10, 2009; DOI: 10.1158/1541-7786.MCR-08-0409

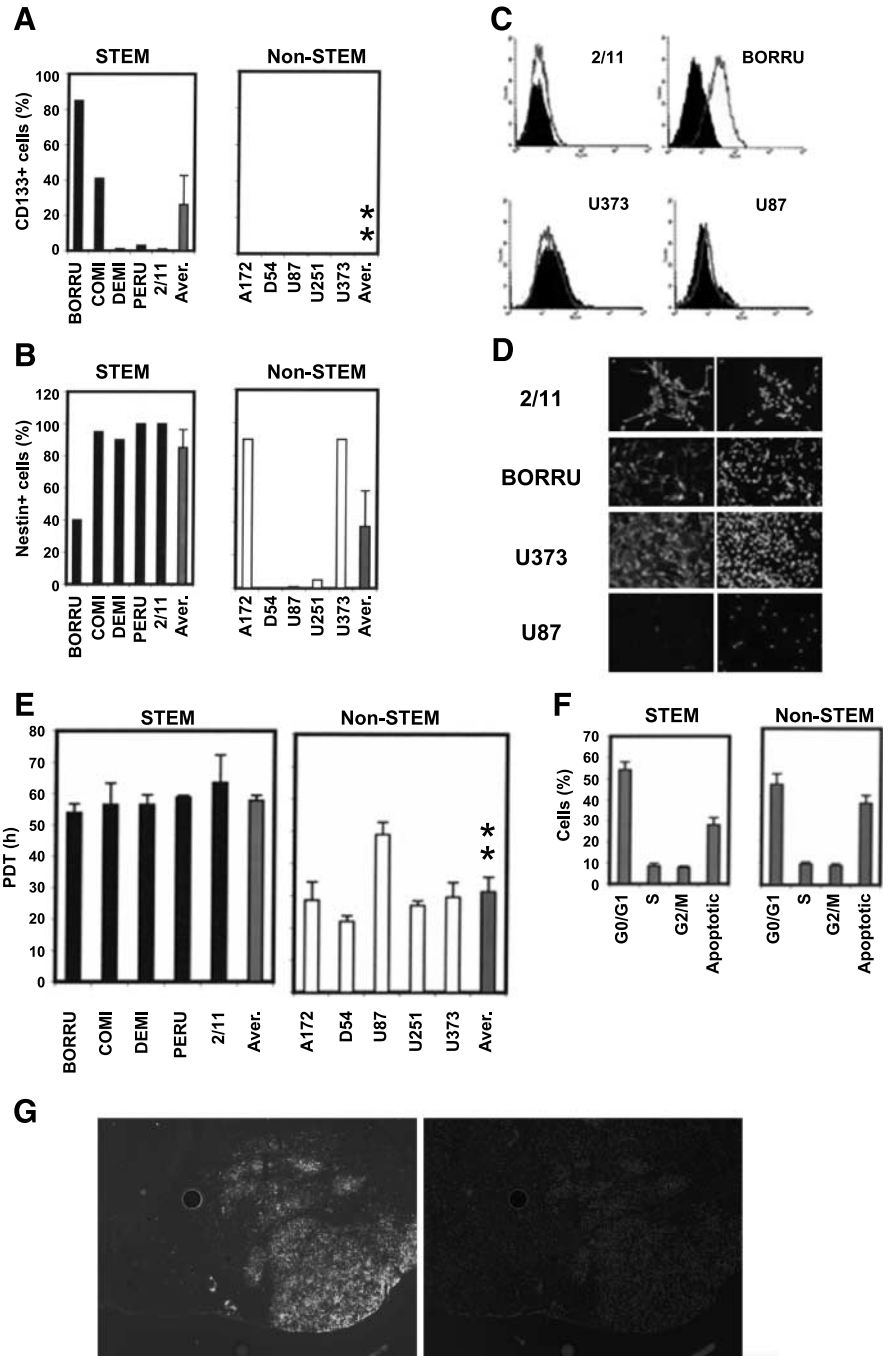

FIGURE 1. Self-renewal of glioma stem cells. **A.** Expression of CD133 in stem (*solid columns*) and nonstem (*open columns*) cells. Cells were incubated with CD133/1-PE antibody and CD133 expression was analyzed on a FACSCalibur. Percentage of positive cells. Average ± SE for stem cells (*far right column*). **, $P < 0.01$, stem versus nonstem cell values (zero). **B.** Expression of nestin in stem and nonstem cells. Cells plated onto Matrigel-coated glass coverslips were fixed and stained with an anti-nestin mouse monoclonal primary antibody and a FITC-conjugated goat anti-mouse secondary IgG. Cells were counterstained with Hoechst 33342 dye to identify all nuclei. Percentage of nestin-positive cells. Average ± SE for stem and nonstem cells (*far right column*). **C.** CD133 fluorescence-activated cell sorting analysis of four representative cell lines: 2/11 and BORRU (stem) an d U373 and U87 (nonstem). **D.** Nestin immunostaining of four representative cell lines: 2/11 and BORRU (stem) and U373 and U87 (nonstem). **E.** PDT of stem (*solid columns*) and nonstem (*open columns*) cells. Appropriate numbers of cells were seeded and grown for 7 to 21 d. Total number of cells was then counted, and after determination of the plating efficiency, the population doublings were calculated according to ref. 31). Mean ± SE number of hours required to double the cell population. Average ± SE for five stem and nonstem cell lines (*far right column*). **, $P < 0.01$, nonstem versus stem cells. **F.** Cell cycle distribution and apoptotic cells in stem (*left*) and nonstem (*right*) cells. Cells were harvested, permeabilized, incubated with propidium iodide, and analyzed on a FACSort cytofluorimeter. Based on propidium iodide staining, cells were defined as G_0-G_1 (DNA content = n), G_2-M (DNA content = 2n), S (n < DNA content < 2n), or apoptotic (DNA content < n). Average ± SE for five cell lines. **G.** Representative image of a stem cell-driven tumor. 10^5 COMI cells were injected in the left corpus striatum of NOD/SCID mice. Four months later, animals were sacrificed and brains were fixed and stained with an anti-nestin mouse monoclonal primary antibody and a FITC-conjugated goat anti-mouse secondary IgG (*left*) and counterstained with Hoechst 33342 dye to identify all nuclei (*right*).

Published OnlineFirst March 10, 2009; DOI: 10.1158/1541-7786.MCR-08-0409

Table 1. Cancer-Initiating Ability on Orthotopic Implantation

Stem	No. Injected Cells	Tumor	Reference	Nonstem	No. Injected Cells	Tumor	Reference
BORRU	10^5	+	This study	A172	$>10^8$	–	(11-14)
COMI	10^5	+	This study	D54	10^4-5 × 10^7	+	(11-14)
DEMI	10^5	+	This study	U87	5 × 10^5	+	(15)
PERU	10^5	+	This study	U251	10^4-5 × 10^7	+	(11-13)
2/11	10^5	+	This study	U373	10^4-5 × 10^7	+	(11-14)

DNA Repair

BER. Figure 4A to C compare the BER capacities of stem and nonstem cells. BER was determined by an *in vitro* assay in which plasmid substrates containing a single AP site at a defined location are repaired by mammalian cell extracts (16). The repair of AP sites is usually accomplished within 60 min incubation time. pGEM U (ung) plasmid substrates containing a single AP site at a defined location were incubated for 30 min (Fig. 4A) and 60 min (Fig. 4B) with 30 μg of the indicated stem (*solid columns*) or nonstem (*open columns*) cell extracts in the presence of [^{32}P]dTTP. A 25-mer *Sma*I-*Pst*I fragment encompassing the lesion (Fig. 4C) was then resolved by denaturing PAGE and repair incorporation was quantified by phosphorimaging analysis. The average repair capacities of stem and nonstem lines did not differ significantly at either 30 min (Fig. 4A; 174 ± 54 and 187 ± 101 [^{32}P]dTMP incorporated dpm, respectively) or 60 min (Fig. 4B; 189 ± 43 and 296 ± 140 [^{32}P]dTMP incorporated dpm, respectively) incubation times. Thus, stem cells do not have increased BER capacity compared with nonstem cells. In particular, no correlation with CD133 or nestin expression was observed. A representative experiment done with two stem (BORRU and 2/11) and two nonstem (U87 and U373) cell lines with different expression levels of CD133 and nestin (Fig. 1A-D) is shown in Fig. 4C. BORRU cell extracts with high CD133 expression (Figs. 4C, *lanes 1* and *2*, and 1A) had lower BER capacity than 2/11 extracts with low CD133 expression (Figs. 4C, *lanes 3* and *4*, and 1A). Likewise, U373 extracts with elevated nestin expression (Figs. 4C, *lanes 7* and *8*, and 1B) had lower BER capacity than U87 extracts with low nestin expression (Figs. 4C, *lanes 5* and *6*, and 1B). As a control, undamaged pGEM T plasmids did not incorporate any labeled nucleotide in the analyzed region (Fig. 4C, *lanes 9-12*).

Resolution of pH2AX Nuclear Foci after IR. H2AX has been identified as one of the key histones to undergo various post-translational modifications in response to DNA DSB. DSB

Table 2. Karyotypic Alterations

Chr	Stem						Nonstem					
	BORRU	COMI	DEMI	PERU	2/11		A172	D54	U87	U251	U373	
	60,XXYY	48-49,XXY	47-48,XY	83-94,XXYY	94-96,XXYY		70-79,XYY	56-68,X	43-44,X	68-76,XX	61-75,XXY	
X		+p−						−				
Y								−		−	t(Y;1)	
1	−(a)	t(1;1)		+	−;t(1;?)		−;t(1;?)	p−	t(1;?);q−	ip;+p+;+p+/−	t(1;?)	
2	−		+	−	inv p		dup q	t(2;4)	p−		−	
3	−			+	t(3;?)		p-;q+	−		t(3;3;?)	t(3;16)	
4	−		+				−	−		−	−	
5	−;p+(b)						−			+	p+;q−	
6	q-;t(?;6)			−			−	−	t(6;?)			
7	−		+	+	+		q−	p−		+	+	
8	−	−		+;−	−			−			p+;t(8;9)	
9	p−	t(8;9);p−			+;−		−	−	p−	q−		
10	−	t(7;10)	−	−	p−		+	q−		−	t(10;18)	
11		p+		p−			t(11;11)	p-/q−	−	+t(11;15);+q-;	t(11;?)	
12				+;−				p−	q−	+t(11;?);iq	−	
13	−		t(13;14)	−				+	−;dup q	−	−	
14	−			−			−	−	−	q−	−;q+	
15	−				−			−		−		
16					t(16;21)		+	q−	t(1;16)		−	
17	t(17;?)			−			+	p−			+	
18					+		−	−			−	
19	−		+	−	+		−	−				
20			+	+;−	+		+	+	t(13;20)			
21				+			+	+			+	
22	−			+	+			−	+			
	No. structural aberrations/cell line					Total stem	No. structural aberrations/cell line					Total nonstem
	5	6	1	1	5	18	6	9	9	10	10	44
	No. numerical aberrations/cell line					Total stem	No. numerical aberrations/cell line					Total nonstem
	13	2	6	18	10	49	13	13	4	12	10	52

NOTE: (a) −, loss; +, gain of whole chromosome. (b) p+;q+, addition; p−;q−, deletion.

Published OnlineFirst March 10, 2009; DOI: 10.1158/1541-7786.MCR-08-0409

caused by IR result in rapid phosphorylation of H2AX at Ser^{139} by ATM protein (17). pH2AX localizes to sites of DSB at subnuclear foci that can be conveniently visualized by immunofluorescence (18). Figure 4D shows the resolution of pH2AX nuclear foci in $CD133^+$ and matched $CD133^-$ BORRU glioma cells after 3 Gy IR. The percentage of cells with nuclear foci of pH2AX after IR was not significantly different in $CD133^-$ and $CD133^+$ cells at both 1 and 24 h after treatment (Fig. 4D).

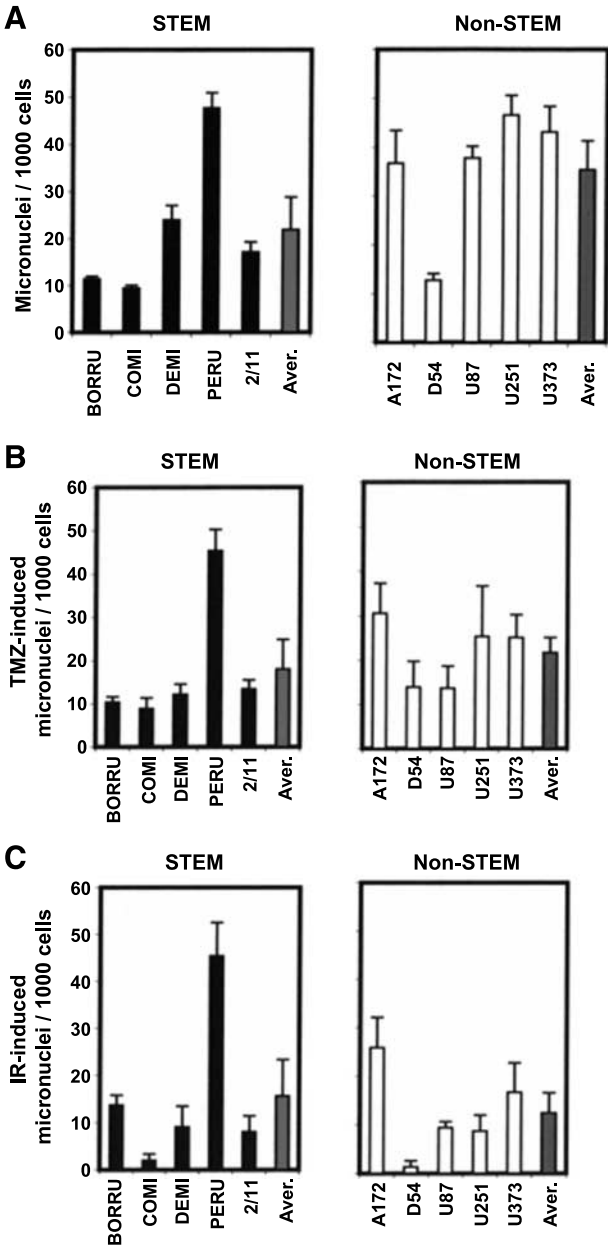

FIGURE 2. Micronuclei in glioma stem cells. **A.** Spontaneous micronuclei determined by scoring 3,000 Giemsa-stained cells by light microscopy. Mean ± SE number of micronuclei/1,000 cells in stem (*solid columns*) and nonstem (*open columns*) cells. Average ± SE for five stem and nonstem cell lines (*far right columns*). **B.** Temozolomide-induced micronuclei. Cells were exposed to 200 μmol/L temozolomide in medium without serum, washed with PBS, and re-fed with complete medium. Eight days later, cells were fixed and stained and 3,000 cells were scored by light microscopy. Spontaneous frequencies were subtracted. Mean ± SE number of micronuclei/1,000 cells in stem (*solid columns*) and nonstem (*open columns*) cells. Average ± SE for five stem and nonstem cell lines (*far right columns*). **C.** IR-induced micronuclei in stem (*solid columns*) and nonstem (*open columns*) cells. Cells were exposed to 0.24 Gy IR in medium without serum and micronuclei analysis was done as described in **B**.

Table 3. Capacity to Generate Nontumorigenic End Cells

Stem	$CD133^+$		$CD133^-$	
	No. Injected Cells	Tumor	No. Injected Cells	Tumor
BORRU	10^4	+	10^5	–
COMI	10^3	+	10^5	–
DEMI	10^4	+	10^5	–
PERU	10^4	+	10^5	–
2/11	10^4	+	10^5	–

Single-Cell Gel Electrophoresis. An increased strand break repair capacity determined by single-cell gel electrophoresis has been reported by Bao et al. (6) in $CD133^+$ versus $CD133^-$ cells of primary glioma T3539 cells and D456MG xenograft cells. We have similarly investigated the SSB repair capacity of purified $CD133^+$ and $CD133^-$ cells isolated from BORRU and COMI stem cell lines (ref. 19; Fig. 4E). We found no significant difference of SSB repair capacity between $CD133^+$ and $CD133^-$ cells at all investigated repair times (1, 18, and 28 h).

Chk1 and Chk2 Activation. Chk1 kinase acts downstream of ATM/ATR kinase to play an important role in DNA damage checkpoint control and tumor suppression (20). Activation of Chk1 involves phosphorylation of Ser^{345} and other sites and occurs in response to genotoxic stress and blocked DNA replication. Chk2 is the mammalian orthologue of the budding yeast Rad53 and fission yeast Cds1 checkpoint kinases. After DNA damage, ATM/ATR phosphorylates Ser^{19} and other sites in the amino-terminal domain of Chk2, a region with cell cycle regulatory function (21). We examined the activation of Chk1 and Chk2 in $CD133^+$ and $CD133^-$ BORRU cells by Western blotting analysis (Fig. 5). Consistent with the elongated cell cycle of STEM cells (Fig. 1E), we observed an increased activation of Chk1 and Chk2 in untreated $CD133^+$ compared with $CD133^-$ cells. Hence, $CD133^+$ cells display enhanced basal activation of checkpoint kinases that may determine their cell cycle delay and contribute to their radioresistance by allowing more time for DNA repair of damages.

Discussion

Characterization of Glioma Stem Cells

Vescovi et al. (7) have proposed five cardinal features to define brain tumor stem cells according to generally accepted criteria. We briefly discuss them in the light of our findings.

Extensive Cell Renewal Ability. It was shown *ex vivo* in stem cells used in this study by population kinetic analyses (PDT and cell cycle distribution; Fig. 1). By definition yet, it features immortal nonstem cell lines too.

Cancer-Initiating Ability on Orthotopic Implantation. It has been reported that stem cells may persist in established malignant cell lines such as the C6 glioma cell line and that those subpopulations of stem cells would be crucial for malignancy (22). However, three of five established cell lines analyzed in this study (D54, U87, and U251) contained no

Published OnlineFirst March 10, 2009; DOI: 10.1158/1541-7786.MCR-08-0409

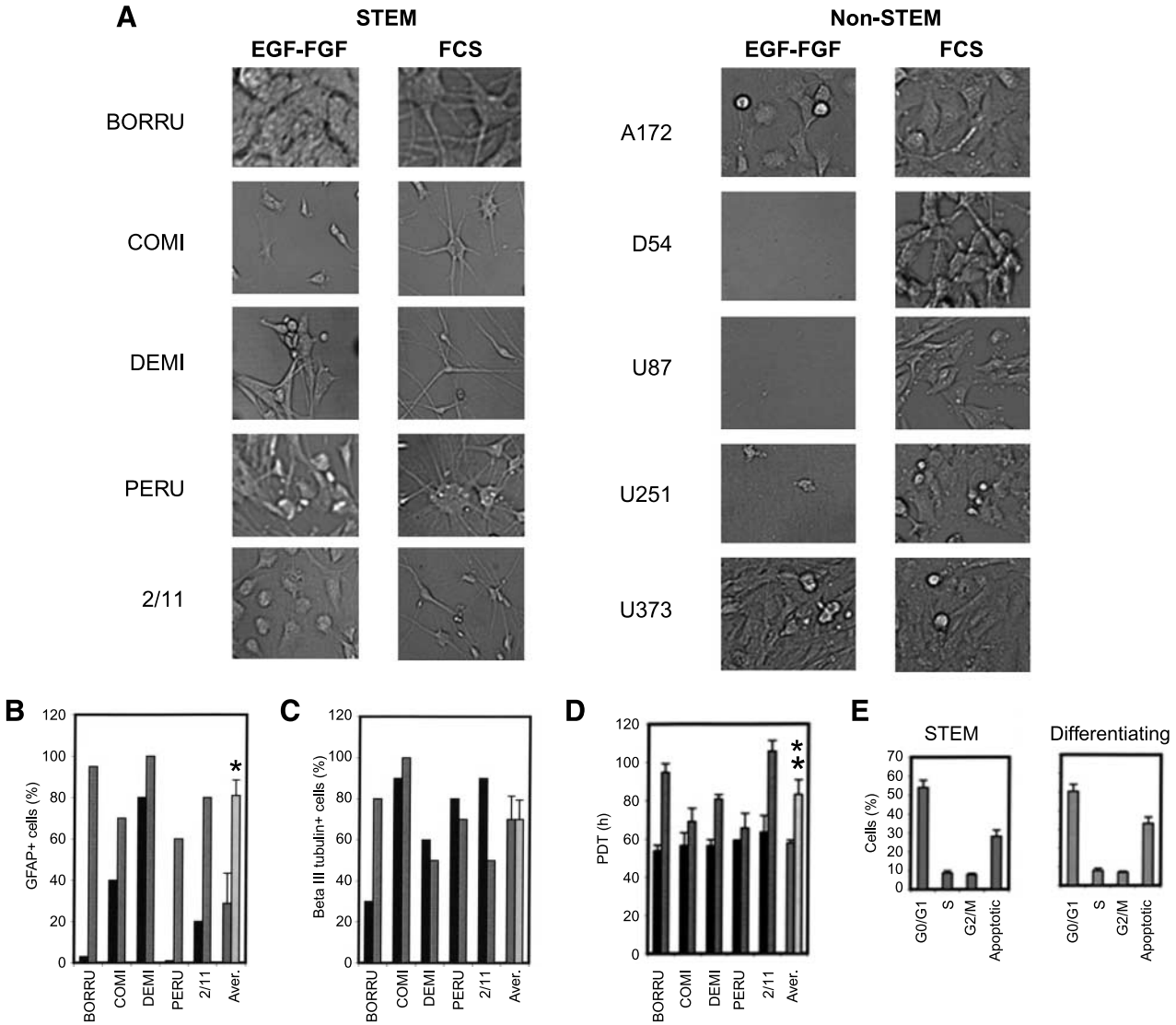

FIGURE 3. Differentiation of glioma stem cells. **A.** Morphology of stem (*left*) and nonstem (*right*) cells. Cells were cultured in the presence of EGF-FGF (stem conditions) or FCS (differentiating conditions) for 21 d and their morphology was photographed with an inverted microscope. **B.** Expression of GFAP in stem (*solid columns*) and differentiating (*gray columns*) cells. Cells plated onto Matrigel-coated glass coverslips were fixed and stained with an anti-GFAP rabbit polyclonal primary antibody and a rhodamine-conjugated goat anti-rabbit secondary IgG. Cells were counterstained with Hoechst 33342 dye to identify all nuclei. Percentage of positive cells. Average for five stem and differentiating cell lines (*far right columns*). *, $P < 0.05$. **C.** Expression of β-tubulin III in stem (*solid columns*) and differentiating (*gray columns*) cells. Cells plated onto Matrigel-coated glass coverslips were fixed and stained with an anti-β-tubulin III mouse monoclonal primary antibody and a FITC-conjugated goat anti-mouse secondary IgG. Cells were counterstained with Hoechst 33342 dye to identify all nuclei. Percentage of positive cells. Average for five stem and differentiating cell lines (*far right columns*). **D.** PDT of stem (*solid columns*) and differentiating (*gray columns*) cells. Appropriate numbers of cells were seeded and grown for 7 for 21 d. Total number of cells was then counted, and after determination of the plating efficiency, the population doublings were calculated according to ref. 31). Mean number ± SE of hours required to double the cell population. Average ± SE for five stem and differentiating cell lines (*far right columns*). **, $P < 0.01$. **E.** Cell cycle distribution and apoptotic cells in stem (*left*) and differentiating (*right*) cells. Cells were harvested, permeabilized, incubated with propidium iodide, and analyzed on a FACSort cytofluorimeter. Based on propidium iodide staining, cells were defined as G_0-G_1 (DNA content = n), G_2-M (DNA content = 2n), S (n < DNA content < 2n), or apoptotic (DNA content < n). Average ± SE for five cell lines.

$CD133^+$ cells as detectable with our gold standard FACSCalibur system (Fig. 1), were unable to proliferate under stem cell culture conditions, and showed no differentiation capacity (Fig. 3). Nevertheless, these established cell lines are tumorigenic in the mouse (Table 1, *right*). The general validity of the cancer stem cell hypothesis has been recently questioned with different points, including the observation that the low frequency of tumor-sustaining cells observed in xenotransplantation studies may reflect the limited ability of human tumor cells to adapt to growth in a foreign (mouse) milieu (23-25). Our data do not support the hypothesis that cancer-initiating ability on orthotopic implantation is a hallmark of stem cells only at least as defined by Vescovi et al. (7).

Karyotypic or Genetic Alterations. Elevated frequencies of chromosomal aberrations and micronuclei were found in both stem and nonstem cultures (Table 2; Fig. 2). Definitely, they are not a prerogative of cancer stem cells.

Published OnlineFirst March 10, 2009; DOI: 10.1158/1541-7786.MCR-08-0409

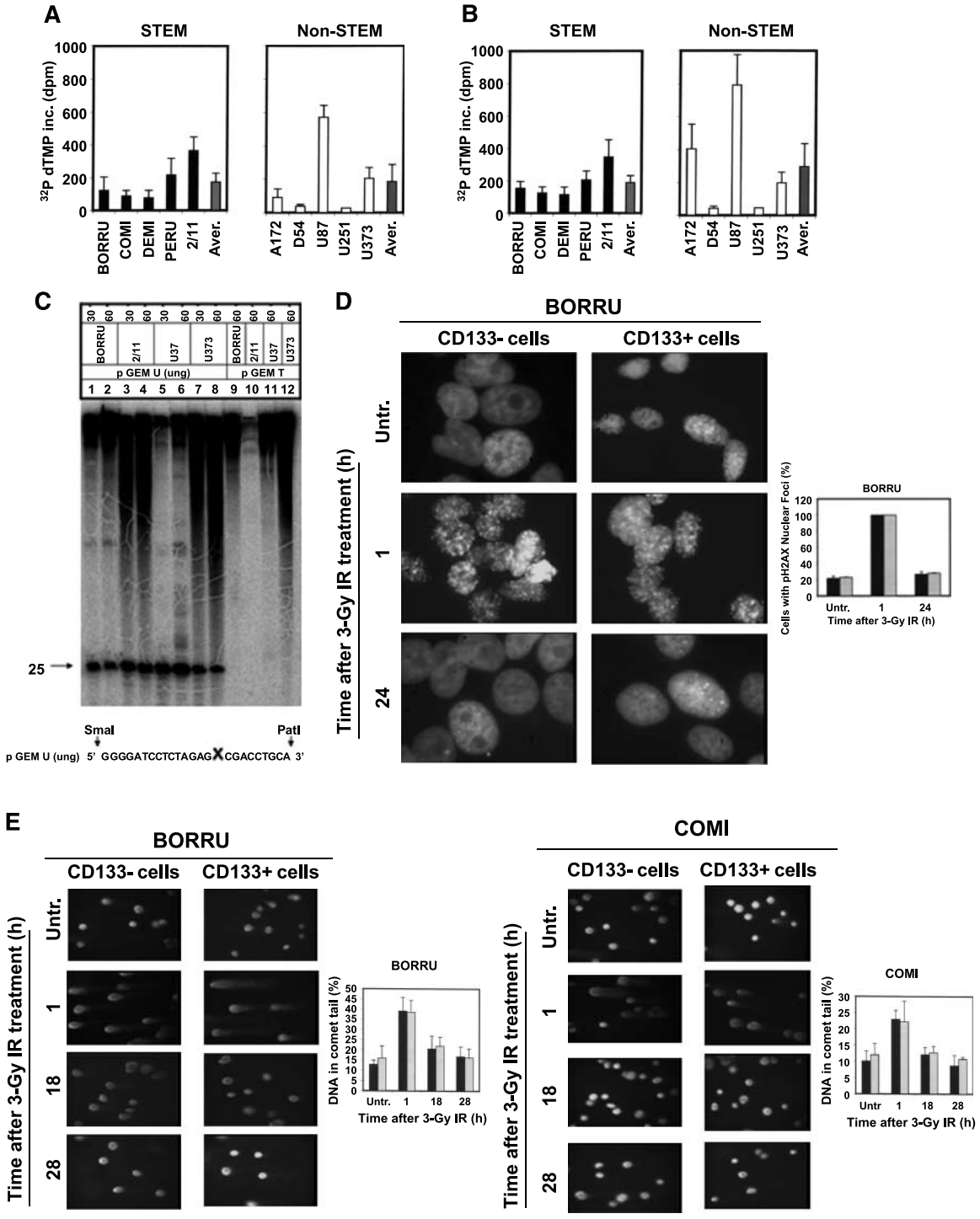

FIGURE 4. DNA repair in glioma stem cells. **A** to **C.** BER in stem (*solid columns*) and nonstem (*open columns*) cells. pGEM U (ung) plasmid substrates containing a single AP site at a defined location were incubated for 30 and 60 min with 30 μg of the indicated stem (*solid columns*) or nonstem (*open columns*) cell extracts in the presence of [^{32}P]dTTP. The 25-mer *Sma*I-*Pst*I fragment encompassing the lesion was then resolved by denaturing PAGE and repair incorporation was quantified by imaging analysis. Average ± SE for five stem and nonstem cell lines (*far right columns*). **A.** 30 min incubation time. **B.** 60 min incubation time. **C.** Representative experiment with two stem (BORRU and 2/11) and two nonstem (U87 and U373) cell extracts. *Bottom, Sma*I-*Pst*I analyzed fragment; *X,* AP site. **D.** Resolution of pH2AX foci. CD133$^+$ (*dark columns in histogram*) and CD133$^-$ (*light columns in histogram*) cells derived from BORRU glioma were grown under control conditions or irradiated with 3 Gy IR and then assessed at 1 and 24 h after irradiation for pH2AX foci. Cells were pemeabilized, immunoblotted with an anti-pH2AX monoclonal antibody conjugated with a fluorochrome, and visualized under a fluorescence microscope. Percentages of CD133$^-$ and CD133$^+$ cells with nuclear foci of pH2AX were then quantified (mean ± SE; n = 100 cells × 3 trials). Left, representative images of cells with pH2AX foci under untreated control or IR treatment conditions. **E.** SSB repair in CD133$^+$ and CD133$^-$ cells. CD133$^+$ (*dark columns in histogram*) and CD133$^-$ (*light columns in histogram*) BORRU (*left*) or COMI (*right*) cells were separated and plated. Sixteen hours later, adherent cells were irradiated with 3 Gy IR and SSB repair was assessed by measuring the percentage of DNA in comets' tails at the indicated repair times.

Published OnlineFirst March 10, 2009; DOI: 10.1158/1541-7786.MCR-08-0409

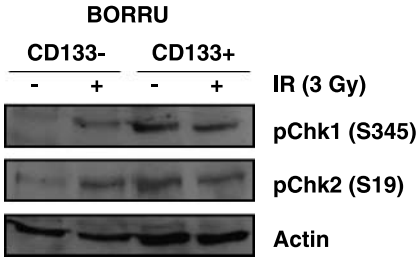

FIGURE 5. Chk1 and Chk2 activation in $CD133^+$ and $CD133^-$ cells. The phosphorylated state of the Chk1 (Ser^{345}) and Chk2 (Ser^{19}) checkpoint kinases was assessed in BORRU $CD133^+$ and $CD133^-$ cells without (-) and 1 h after IR treatment (+). Whole-cell lysates were prepared, resolved by SDS-PAGE, and immunoblotted with primary rabbit polyclonal antibodies raised against phospho-Chk1 (Ser^{345}) and phospho-Chk2 (Ser^{19}). Immunoblotting for actin served as a loading control.

Capacity to Generate Nontumorigenic End Cells. It featured stem cells, where CD133 expression correlates with tumorigenicity (Table 3), but was not determinable in nonstem cells, due to the lack of expression of CD133 in them. Because no alternative marker is currently available to distinguish tumorigenic from nontumorigenic nonstem cells, it is not possible to show inability to generate the latter.

Differentiation Capacity. It was the watershed between stem and nonstem cells in this study. Acquisition of astroglial morphology and expression of astroglial differentiation markers were peculiar to stem cells only (Fig. 3). This was accompanied by a significant elongation of PDT and cell cycle phases. In our opinion, the term cancer "stem" cell should be applied to cancer-driving cells only in case of differentiation capacity. Otherwise, the term "cancer-initiating cell" or "tumor-propagating cell" could be more appropriate (23-25).

In conclusion, we found the defining features of brain tumor stem cells proposed by Vescovi et al. (7) a valuable tool to standardize and guide work in the field. We would further emphasize that the differentiation capacity may be considered as an indispensable feature to talk about "stem" cells. In the presence of such a hallmark, whether the term "cancer" may further be applied would depend on fulfillment of all additional criteria proposed by Vescovi et al. (7).

DNA Repair

The contribution of DNA repair to resistance of cancer stem cells to radiotherapy or chemotherapy is poorly defined (26). It has been reported that cancer stem cells contribute to glioma radioresistance through preferential activation of the DNA damage checkpoint response and an increase in DNA repair capacity as measured by the single-cell gel electrophoresis assay and resolution of pH2AX foci (6). In our study, the PDT was longer (Fig. 1E) in stem compared with nonstem cells, and activation of Chk1 and Chk2 checkpoint kinases was more pronounced in $CD133^+$ compared with $CD133^-$ cells even in the absence of treatment (Fig. 5), indicating that delayed cell cycle may represent a general mechanism of genome safeguard in glioma stem cells, allowing these cells more time to repair DNA damage.

Neither BER or SSB repair visualized by the comet assay nor resolution of pH2AX foci, an indicator of DSB repair, was enhanced in $CD133^+$ cells (Fig. 4). Thus, although stem cells display peculiar features of proliferation and constitutive activation of checkpoint kinases that may contribute to their resistance to therapeutic agents, no enhancement of DNA repair capacity could be observed in them. The inconsistency with the increased SSB and DSB repair capacity reported by Bao et al. (6) in $CD133^+$ cells of primary glioma T3539 cells and D456MG xenograft cells may indicate the dependency of this phenomenon on the glioma stem line under use and may not represent a common feature of glioma stem cell lines.

Materials and Methods

Cell Lines

Surgery-derived tumor specimens were obtained, after informed consent, from five male patients with diagnosis of glioblastoma multiforme, WHO grade IV. They were collected on ice and immediately processed for isolation of stem cells according to Svendsen et al. (27) with modifications. Briefly, tissue was washed, minced, and triturated and cells were seeded at a concentration of 100,000/mL into tissue culture flasks coated with Matrigel (BD Biosciences). Cells were grown in proliferation medium containing DMEM/F-12/NSA and N2 supplement (1:50; Life Technologies/Invitrogen), recombinant human FGF-2 (10 ng/mL; Peprotech), and recombinant human EGF (20 ng/mL; Peprotech). Fresh FGF-2 and EGF were added twice per week. Under these conditions, the cells attach and grow as a monolayer in flasks and maintain intact self-renewal capacity for at least 3 months. Removal of growth factors and addition of 10% FCS to the proliferation medium results after ~3 weeks in acquisition of astroglial morphology and expression of the differentiation marker GFAP (Fig. 3).

The established cell lines A172, D54, U87, U251, and U373 were used as nonstem controls. All these lines derive from WHO grade IV glioblastoma multiforme tumors (11-15). A172, D54, and U87 cells are wild-type for p53. U251 and U373 are p53 mutant. D54 and U251 cells were kind gifts of Prof. P. Quesada (University of Naples). A172 and U373 were kind gifts of Prof. T. Florio (University of Genova). U87 was purchased from the Interlab Cell Line Collection at Istituto Nazionale Ricerca Cancro. All nonstem cell lines were cultured in DMEM containing 10% FCS unless otherwise indicated.

Tumorigenicity

Tumorigenicity in NOD/SCID mice was used to check that the stem cells maintained brain tumor-initiating activity. For intracranial inoculation, two to four NOD/SCID mice (6-8 weeks old; Charles River) were anesthetized with i.m. ketamine and xylazine. Thereafter, the animals were positioned into a stereotaxic frame (David Kopf instruments) and a hole was made using a 21-gauge needle, 2.5 mm lateral and 1 mm anterior from the intersection of the coronal and sagittal sutures (bregma). The indicated number of cells was injected in the left corpus striatum. Animals were observed for at least 6 months for progressive tumor growth at the site of injection. For tumor analysis, animals were sacrificed and brains were fixed and stained with an anti-nestin mouse monoclonal primary antibody and a FITC-conjugated goat anti-mouse secondary IgG and counterstained with Hoechst 33342 dye to identify all nuclei. Progressive tumor growth was defined by the ability of the

Published OnlineFirst March 10, 2009; DOI: 10.1158/1541-7786.MCR-08-0409

tumors to enlarge continuously and be serially transplanted. All experiments including animals were done in compliance with guidelines approved by the Ethical Committee for Animal Use in Cancer Research at Istituto Nazionale Ricerca Cancro.

Morphologic and Marker Analysis

Cells were cultured in the presence of growth factors (stem conditions) or FCS (differentiating conditions) for 21 days and photographed with an inverted microscope (Olympus Biosystems) in transmitted light.

CD133 expression was determined as follows. Adherent cells were removed with 0.5 mmol/L EDTA in PBS, washed, suspended in buffer (2% bovine serum albumin in PBS), and incubated with CD133/1-PE (Miltenyi Biotech) or isotype control antibody (IgG1-PE; Miltenyi Biotech). CD133 expression was analyzed on a FACSCalibur (BD Biosciences). For immunostaining, the cells plated onto Matrigel-coated glass coverslips were fixed with 4% paraformaldehyde for 15 min at room temperature, treated with PBS-10% FCS-0.3% Triton X-100, and then stained with the following antibodies: anti-nestin (mouse monoclonal; 1:1,000; Novus Biologicals), anti-β-tubulin III (mouse monoclonal; 1:10,000; Sigma), and anti-GFAP (rabbit polyclonal; 1:10,000; DAKO). The primary antibodies were detected with FITC-conjugated goat anti-mouse IgG (1:700; Alexa) and rhodamine-conjugated goat anti-rabbit IgG (1:250; Jackson ImmunoResearch). The cells were counterstained with Hoechst 33342 dye (Sigma) to identify all nuclei. Quantification of cells positive for a specific marker was carried out by counting all the stained cells within 20 randomly selected microscope fields per specimen, and the percentage was calculated based on the total number of nuclei counted.

$CD133^+$ cells were purified by CD133/1 Miltenyi microbeads as per manufacturer instructions (Miltenyi Biotech). Cells were dissociated and resuspended in PBS containing 0.5% bovine serum albumin and 2 mmol/L EDTA. Positive magnetic cell separation was done using two magnetic cell separation columns in series. Aliquots of $CD133^+$ and $CD133^-$ cells were evaluated for purity by flow cytometry using CD133/2-PE (Miltenyi Biotech) or isotype control antibody (IgG2b-PE; Miltenyi Biotech) and analyzed on a BD FACSCalibur. Percentages of purified $CD133^+$ and $CD133^-$ cells were $\geq$80% and $\geq$95%, respectively.

Karyotypic Alterations and Micronuclei

The karyotype of stem and nonstem cell lines was analyzed using conventional cytogenetic analysis as described (28). Spontaneous micronuclei were determined as described (29). For temozolomide-induced micronuclei, cells were preliminarily exposed to temozolomide in medium without serum for 2 h, washed, and cultivated in complete medium for 8 days. Micronuclei were then determined after subtraction of spontaneous frequencies. For IR-induced micronuclei, cells were irradiated with 0.24 Gy in suspension by a CIS Bio International IBL437C irradiator. Cells were then plated and cultivated for 8 days and micronuclei were determined as above.

Cell Cycle Analysis, Apoptosis, and PDT

Cell cycle and apoptosis were analyzed as described (30). PDT was determined according to Glaab and Tindall (31).

BER

The BER pathway was analyzed on plasmid substrates containing a single AP site as described (16). Briefly, extracts prepared by the method of Tanaka et al. (32) were incubated with 400 ng plasmid substrate in the presence of [^{32}P]dTTP (GE Healthcare). DNA was then purified and treated with restriction endonucleases *Sma*I-*Pst*I and the 25-mer fragment was resolved by denaturing PAGE. [^{32}P]dTMP incorporation was quantified by a Typhoon 9200 variable mode imager (Molecular Dynamics).

Resolution of pH2AX Foci

Matched $CD133^-$ and $CD133^+$ tumor cell cultures were purified (see Morphologic and Marker Analysis) from BORRU glioma and grown under control conditions or irradiated with 3 Gy IR and then assessed at 1 and 24 h after irradiation. Cells were pemeabilized, immunoblotted with an anti-pH2AX (Ser^{139}) rabbit monoclonal antibody conjugated with Alexa Fluor 488 (Cell Signaling Technology), and visualized under a fluorescence microscope. The percentage of $CD133^-$ and $CD133^+$ cells with nuclear foci of pH2AX was quantified after scoring 100 cells.

Single-Cell Gel Electrophoresis

Single-cell gel electrophoresis was carried out as described (19). Briefly $CD133^+$ and $CD133^-$ cells were separated and plated. The following day, adherent cells were irradiated with 3 Gy IR and SSB repair was assessed by measuring the percentage of DNA in comets' tails at the indicated repair times.

pChk1 and pChk2 Assay In vitro

$CD133^+$ and $CD133^-$ cells isolated from BORRU tumor were treated with IR (3 Gy) to induce DNA damage. The activation state of the checkpoint response was assessed 1 h later. Cells were extracted with lysis buffer [50 mmol/L Tris-HCl (pH 7.4), 1 mmol/L EDTA, 100 mmol/L NaCl, 0.1% NP-40, 6 mmol/L EGTA] supplemented with phosphatase inhibitors (PhosSTOP; Roche) and protease inhibitors (Complete, Mini; Roche). Western blot analysis for detecting the pChk1 and pChk2 proteins was done by using primary rabbit polyclonal antibodies raised against pChk1 (Ser^{345}) and pChk2 (Ser^{19}) as per manufacturer's instructions (Cell Signaling Technology).

Statistical Analysis

The two-tailed nonparametric Mann-Whitney test was used. Statistical analysis was done using the statistical software GraphPad Instat 3.0 for Windows. Statistical significance was indicated with one ($P < 0.05$) or two ($P < 0.01$) asterisks.

Disclosure of Potential Conflicts of Interest

No potential conflicts of interest were disclosed.

References

1. Hambardzumyan D, Squatrito M, Carbajal E, Holland EC. Glioma formation, cancer stem cells, and Akt signaling. Stem Cell Rev 2008;4:203–10.

2. Eramo A, Ricci-Vitiani L, Zeuner A, et al. Chemotherapy resistance of glioblastoma stem cells. Cell Death Differ 2006;7:1238–41.

Published OnlineFirst March 10, 2009; DOI: 10.1158/1541-7786.MCR-08-0409

3. Murat A, Migliavacca E, Gorlia T, et al. Stem cell-related "self-renewal" signature and high epidermal growth factor receptor expression associated with resistance to concomitant chemoradiotherapy in glioblastoma. J Clin Oncol 2008; 26:3015–24.

4. Jin F, Zhao L, Zhao HY, et al. Comparison between cells and cancer stem-like cells isolated from glioblastoma and astrocytoma on expression of anti-apoptotic and multidrug resistance-associated protein genes. Neuroscience 2008;154:541–50.

5. Kang MK, Kang SK. Pharmacologic blockade of chloride channel synergistically enhances apoptosis of chemotherapeutic drug-resistant cancer stem cells. Biochem Biophys Res Commun 2008;373:539–44.

6. Bao S, Wu Q, McLendon RE, et al. Glioma stem cells promote radioresistance by preferential activation of the DNA damage response. Nature 2006;444:756–760.

7. Vescovi AL, Galli R, Reynolds BA. Brain tumour stem cells. Nat Rev Cancer 2006;6:425–436.

8. Beier D, Hau P, Proescholdt M, et al. CD133(+) and CD133(-) glioblastoma-derived cancer stem cells show differential growth characteristics and molecular profiles. Cancer Res 2007;67:4010–5.

9. Günther HS, Schmidt NO, Phillips HS, et al. Glioblastoma-derived stem cell-enriched cultures form distinct subgroups according to molecular and phenotypic criteria. Oncogene 2008;27:2897–909.

10. Joo KM, Kim SY, Jin X, et al. Clinical and biological implications of CD133-positive and CD133-negative cells in glioblastomas. Lab Invest 2008;88:808–15.

11. Bigner DD, Bigner SH, Pontén J, et al. Heterogeneity of genotypic and phenotypic characteristics of fifteen permanent cell lines derived from human gliomas. J Neuropathol Exp Neurol 1981;40:201–29.

12. Bigner SH, Bullard DE, Pegram CN, Wikstrand CJ, Bigner DD. Relationship of *in vitro* morphologic and growth characteristics of established human glioma-derived cell lines to their tumorigenicity in athymic nude mice. J Neuropathol Exp Neurol 1981;40:390–409.

13. Bullard DE, Schold SC, Jr., Bigner SH, Bigner DD. Growth and chemotherapeutic response in athymic mice of tumors arising from human glioma-derived cell lines. J Neuropathol Exp Neurol 1981;40:410–27.

14. de Ridder LI, Laerum OD, Mørk SJ, Bigner DD. Invasiveness of human glioma cell lines *in vitro*: relation to tumorigenicity in athymic mice. Acta Neuropathol 1987;72:207–13.

15. Li DM, Sun H. PTEN/MMAC1/TEP1 suppresses the tumorigenicity and induces G_1 cell cycle arrest in human glioblastoma cells. Proc Natl Acad Sci U S A 1998;95:15406–11.

16. Frosina G, Cappelli E, Ropolo M, Fortini P, Pascucci B, Dogliotti E. *In vitro* base excision repair assay using mammalian cell extracts. In: Henderson DS, editor. DNA repair protocols: mammalian systems. 2nd ed. Methods in molecular biology. Totowa (NJ): Humana Press; 2006. p. 377–96.

17. Srivastava N, Gochhait S, de Boer P, Bamezai RN. Role of H2AX in DNA damage response and human cancers. Mutat Res 2009;681:180–8.

18. Kinner A, Wu W, Staudt C, Iliakis G. γ-H2AX in recognition and signaling of DNA double-strand breaks in the context of chromatin. Nucleic Acids Res 2008;36:5678–94.

19. Zunino A, Degan P, Vigo T, Abbondandolo A. Hydrogen peroxide: effects on DNA, chromosomes, cell cycle and apoptosis induction in Fanconi's anemia cell lines. Mutagenesis 2001;16:283–8.

20. Enders GH. Expanded roles for Chk1 in genome maintenance. J Biol Chem 2008;283:17749–52.

21. Antoni L, Sodha N, Collins I, Garrett MD. CHK2 kinase: cancer susceptibility and cancer therapy—two sides of the same coin? Nat Rev Cancer 2007;7:925–36.

22. Kondo T. Stem cell-like cancer cells in cancer cell lines. Cancer Biomark 2007;3:245–50.

23. Kelly PN, Dakic A, Adams JM, Nutt SL, Strasser A. Tumor growth need not be driven by rare cancer stem cells. Science 2007;317:337.

24. Hill RP, Perris R. "Destemming" cancer stem cells. J Natl Cancer Inst 2007; 99:1435–40.

25. Adams JM, Strasser A. Is tumor growth sustained by rare cancer stem cells or dominant clones? Cancer Res 2008;68:4018–21.

26. Dean M, Fojo T, Bates S. Tumour stem cells and drug resistance. Nat Rev Cancer 2005;5:275–84.

27. Svendsen CN, Caldwell MA, Ostenfeld T. Human neural stem cells: isolation, expansion and transplantation. Brain Pathol 1999;9:499–513.

28. Viaggi S, Abbondandolo A, Carbone M, et al. Uncommon cytogenetic findings in a case of splenic marginal zone lymphoma with aggressive clinical course. Cancer Genet Cytogenet 2004;148:133–6.

29. Ropolo M, Degan P, Foresta M, et al. Complementation of the oxidatively damaged DNA repair defect in Cockayne syndrome A and B cells by *Escherichia coli* formamidopyrimidine DNA glycosylase. Free Radic Biol Med 2007;42: 1807–17.

30. Poggi A, Pellegatta F, Leone BE. Engagement of the leukocyte-associated Ig-like receptor-1 induces programmed cell death and prevents NF-κB nuclear translocation in human myeloid leukemias. Eur J Immunol 2000; 30:2751–2758.

31. Glaab WE, Tindall KR. Mutation rate at the hprt locus in human cancer cell lines with specific mismatch repair-gene defects. Carcinogenesis 1997;18:1–8.

32. Tanaka M, Lai JS, Herr W. Promoter-selective activation domains in Oct-1 and Oct-2 direct differential activation of an snRNA and mRNA promoter. Cell 1992;68:755–67.

AACR American Association for Cancer Research

Molecular Cancer Research

Comparative Analysis of DNA Repair in Stem and Nonstem Glioma Cell Cultures

Monica Ropolo, Antonio Daga, Fabrizio Griffero, et al.

Mol Cancer Res 2009;7:383-392. Published OnlineFirst March 10, 2009.